

Effects of Crystallization on Cell Morphology in Microcellular Polyphenylene Sulfide

by Masayasu Itoh * and Akira Kabumoto *2

ABSTRACT

Microcellular plastic (MCP) is a polymeric foam with an average cell size of 10 μm or less. The basic process for MCP was proposed in 1981 by Professor Suh at the Department of Mechanical Engineering of MIT in the U.S.¹⁾, and the process has been applied to various plastic materials. In this work, the effects of crystallization of microcellular polyphenylene sulfide (PPS) on its morphology are investigated. When PPS was foamed below its crystallization temperature, a unimodal distribution was observed with a cell size of about 10 μm . When foamed above its crystallization temperature, on the other hand, a bimodal distribution was observed with two peaks at about 10 μm and the submicron order in cell size. It was shown that these submicron-sized cells were generated by cell nucleation induced by crystallization of PPS.

1. INTRODUCTION

Microcellular plastic (hereinafter called MCP) is a polymeric foam with an average cell size of the order of 10 μm or less and a cell density of the $10^9 \sim 10^{15}$ cells/cm³ order. The foam features improved mechanical properties^{2)~4)}, reduced material consumption, decreased dielectric constant⁵⁾ and increased thermal insulation capability, in addition to enhanced light reflecting capability that have been investigated by the authors⁶⁾. The MCP process was originally proposed in 1981 by Professor Suh at the Department of Mechanical Engineering of MIT in the U.S.¹⁾

There are many R&D activities aimed at industrial applications. In this connection, Trexel Inc. in the U.S. has developed the extrusion molding and injection molding processes for MCPs using CO₂ in its supercritical state, and they are promoting licensing of these technologies.

With regard to microcellular foaming behavior using the MCP processes, a broad range of study paper have been presented about the process factors that influence microcellular foaming^{6)~10)}. In cases of crystalline polymers in particular, interesting results have been reported about the correlation between their crystallization and microcellular foaming^{6)~10)}.

In this work, we focused our attention on polyphenylene sulfide (hereinafter called PPS), one of the crystalline polymers provided with superior sliding property and heat resistance, and investigated the effects of its crystallization on the microcellular foaming behavior.

2. BASIC CONCEPT

The basic concept of the MCP process is described in detail in the papers by Professor Suh et al.¹²⁾, and it is shown in Figure 1 schematically.

The process A is characterized by effecting gas saturation at room temperature¹³⁾. More specifically, a solid polymer sheet is saturated with a physical blowing agent of high-pressure inert gas (N₂ or CO₂) at room temperature. To that end, the polymer sheet is kept at rest in the inert gas under a high pressure for sufficient dissolution until a saturated concentration is reached. Then, the gas pressure within the high-pressure vessel is rapidly lowered to atmospheric pressure. Due to this depressurization, the gas dissolved in the solid polymer sheet reaches a super-saturation state thus achieving a thermodynamic instability in the sheet. When the polymer sheet saturated with gas is heated and quenched, microcellular foaming

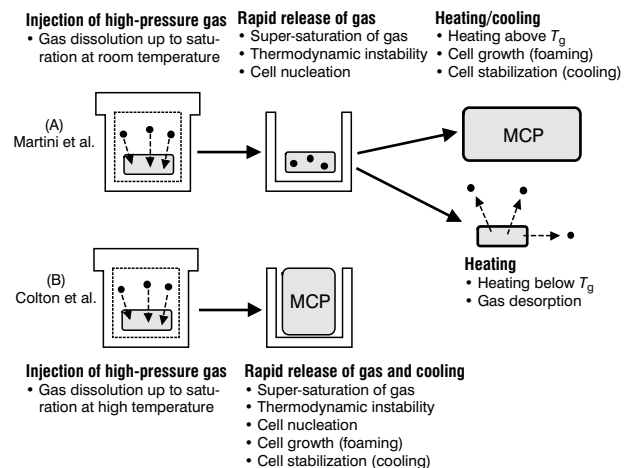


Figure 1 Process for microcellular foaming.

* Polymer Engineering Center, Ecology and Energy Lab., R&D Div.

*2 Production Dept., Foam Products Div., Energy and Industrial Products Co.

occurs, whereby cell nucleation is induced when the temperature reaches just above its glass transition temperature (T_g). Because the dissolved gas induces plasticization of the polymer, however, the cell nucleation is actually induced at a T_g lower than that intrinsic to the polymer. Meanwhile, the plasticization phenomenon becomes the more prominent the higher the dissolved gas concentration, and this phenomenon is accordingly applied in the extrusion of ultra-high-molecular weight polyethylene that has been considered very difficult to be extruded¹⁴⁾.

In the process B¹⁵⁾, on the other hand, after the inert gas is dissolved up to a saturated concentration at higher temperatures, the gas is rapidly removed to simultaneously promote gas super-saturation, cell nucleation and cell growth, thereby obtaining MCP through cooling.

The process B aims at solving the problems that constitute the impediments to practical application of the basic process of batch type such as shortening the gas dissolution time (i.e. increasing the gas diffusion rate by high temperatures) and promoting the dissolution of gas into crystalline polymers. However, from the industrial view point, this process has some problems including the decreased gas uptake and the repetition of heating and cooling cycles of large high-pressure vessels of industrial scale.

In this report, we used the process A above mentioned.

3. EXPERIMENTAL

3.1 Sample

Figure 2 shows the details of the sample used here. The PPS sample is 0.2 mm in thickness, 1.31 g/cm³ in density and about 11 % in crystallinity, i.e. low-crystallinity type.

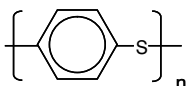
3.2 Experimental Procedure

The experiments were conducted through the process A shown in Figure 1. More specifically, the sample was loaded in a high-pressure vessel, and pressurized by CO₂ for a specified time at room temperature in order to saturate the PPS sample with CO₂. After the specified time elapsed, the pressure was released, and the polymer sample saturated with CO₂ was heated in an air oven of constant temperature to effect foaming, thereby obtaining a polymeric form.

3.3 Evaluation Method of Foamed Polymer

The foamed sample was evaluated as follows.

- Polyphenylene sulfide (PPS)



- Sample sheet used
 - Crystallinity: about 11 %
 - Peak endothermic heat due to 100 % crystal dissolution of PPS : 146.2 J/g
 - Thickness: 0.2 mm
 - Density: 1.31 g/cm³

Figure 2 Polyphenylene sulfide.

3.3.1. Weight Gain due to Gas Saturation

The weight gain due to gas saturation was calculated by the equation below, using electronic balance measurements of the sample weight before loading into the high-pressure vessel for gas saturation W_0 and the sample weight immediately after gas saturation W_1 .

$$\text{Weight gain (wt\%)} = \frac{(W_1 - W_0)}{W_0} \times 100$$

3.3.2. Expansion Ratio

The expansion ratio was calculated by the equation below, using the density of foamed polymer ρ_f measured by the water substitution method and that of non-foamed polymer sheet ρ_0 , i.e. 1.31 g/cm³.

$$\text{Expansion ratio} = \frac{\rho_0}{\rho_f}$$

3.3.3. Cell Morphology

The foamed polymer sample was broken in liquid nitrogen, and the cross-sectional surface was observed using a scanning electron microscope (SEM) for cell morphology.

3.3.4. Crystallinity

A differential scanning calorimeter (DSC) was used to measure the exothermic peak resulting from crystallization and the endothermic peak resulting from crystal dissolution, whereby the crystallinity was calculated by the equation below. The heating rate was set at 10°C/min, and the endothermic peak due to 100 % crystal dissolution of PPS was taken as 146.2 J/g¹⁶⁾.

$$\begin{aligned} \text{Crystallinity} &= \frac{\{(\text{Peak endothermic heat due to crystal dissolution}) \\ &\quad - (\text{Peak exothermic heat due to crystallization})\}}{\text{Peak endothermic heat due to 100 \%} \\ &\quad \text{crystal dissolution (146.2 J/g)}} \\ &\quad \times 100 \end{aligned}$$

4. EXPERIMENTAL RESULTS

4.1 Basic Study of Microcellular Foaming Behavior of PPS

4.1.1. Gas Saturation Behavior

Figure 3 shows the gas saturation curve of PPS/CO₂ system, where three levels of 2.0, 4.0 and 6.5 MPa were selected for the gas pressure. It can be seen that the weight gain of CO₂ gas in the polymer monotonously increased over time for every gas pressure, reaching an equilibrium value in 20 to 30 hr. From these results the relationship between the equilibrium CO₂ concentration and saturation pressure is reduced as shown in Figure 4, whereby it is indicated that the equilibrium gas concentration is in proportion to the saturation gas pressure in accordance with Henry's Law. Based on the results above mentioned, experiments hereafter were conducted while fixing the conditions to 6.5 MPa for gas saturation pres-

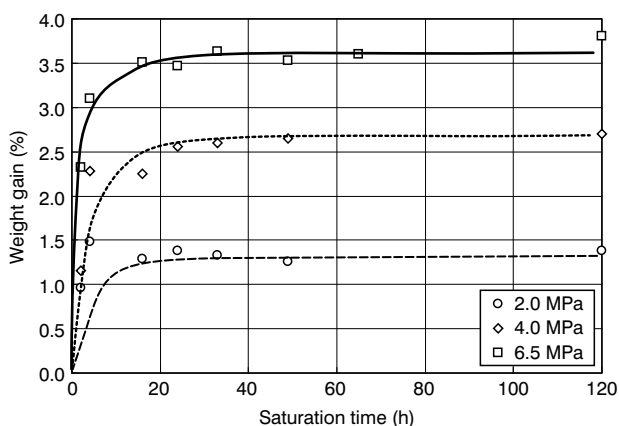


Figure 3 Weight gain for PPS as a function of saturation time.

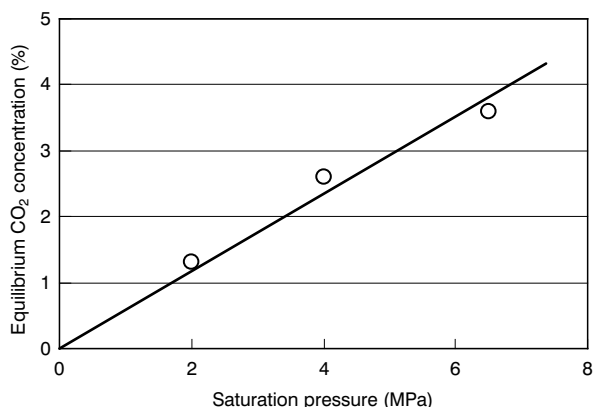


Figure 4 Saturated CO₂ concentration as a function of saturation pressure.

sure and 48 hr for gas saturation time, i.e. sufficient for reaching an equilibrium.

4.1.2. Foaming Behavior

Figure 5 shows the dependence of expansion ratio on foaming time for two foaming temperature levels of 373 K and 473 K. The cell growth is seen to be completed within 60 sec for either foaming temperature. Based on this result, while fixing the foaming time to 60 sec, experiments were carried out to see the dependence of expansion ratio on foaming temperature, and the results are shown in Figure 6. It is observed that, despite the fact that the expansion ratio increases as the foaming temperature rises, it begins to decrease in the vicinity of 410 K in foaming temperature.

Accordingly, we proceeded to observe the changes in cell morphology at each foaming temperature. Figure 7 shows the cross-sectional SEM photographs of foamed PPS for each foaming temperature. As can be seen, while at low foaming temperatures foamed polymers having a single cell size ranging from several to 10 μm are obtained, at higher temperatures of 393 K and beyond a bimodal cell morphology is observed, where cells about 10 μm in size are surrounded by microcells that are orders of magnitudes smaller, i.e. the submicron order. Moreover, as the foaming temperature increases, the volume fraction of the submicron-sized cells increases.

In order to understand such changes in cell morphology, the crystallinity of foamed PPS samples was measured using DSC, and the results are also shown in

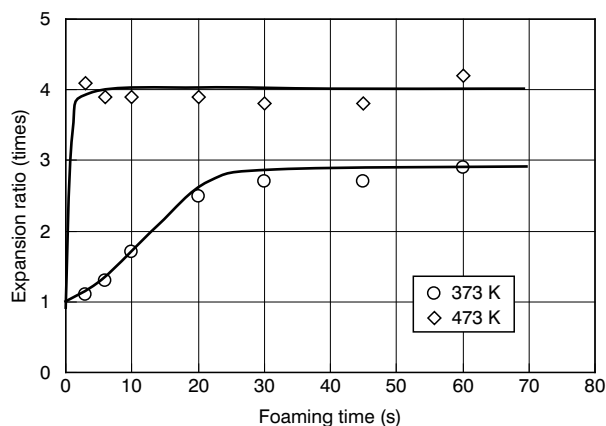


Figure 5 Expansion ratio for PPS as a function of foaming time.

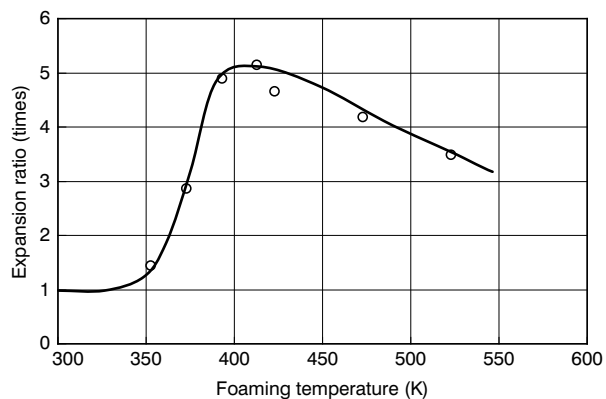
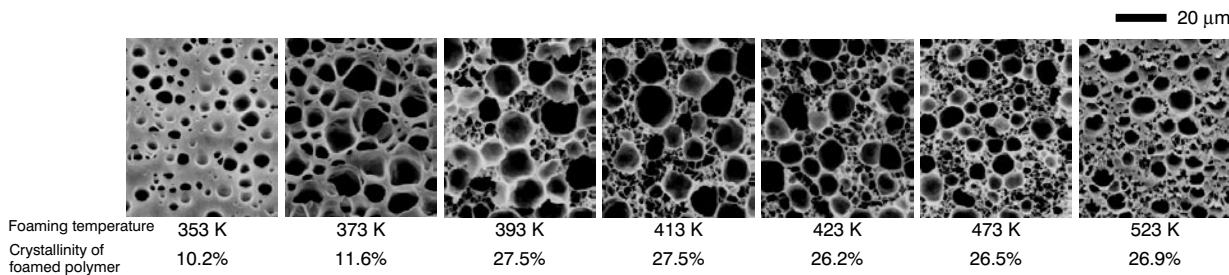


Figure 6 Expansion ratio for PPS as a function of foaming temperature.



Gas concentration: 3.6 wt%, Saturation pressure: 6.5 MPa, Foaming time: 60 sec

Figure 7 Dependence of PPS cell morphology on foaming temperature.

Figure 7. It is seen that the crystallinity of the foamed polymers begins to rise at a temperature where the cell morphology shows a change from single-sized cells to two different-sized cells.

5. DISCUSSIONS

The experimental results suggest that there is a relation of some kind between the foaming behavior and crystallinity of PPS. We investigated therefore the relationship between the crystallization behavior and the cell morphology of microcellular PPS foams.

Figure 8 shows the change in crystallinity associated with gas saturation. It can be seen that in this case of PPS, unlike in the case of polyethylene terephthalate (PET) ⁶⁾, crystallization induced by CO₂ does not occur at the time of gas saturation. On the other hand, from the DSC curve of as-received PPS sheet shown in Figure 9, the thermal crystallization of PPS is seen to begin at about 120°C.

It is thought from these results that the change in cell morphology shown in Figure 7 is affected by the crystallization of PPS induced by heating at the time of foaming, so that we proceeded on further investigations.

5.1 Cell Morphology Change in the Foaming Process

Figure 10 shows the cell morphology in the initiation and

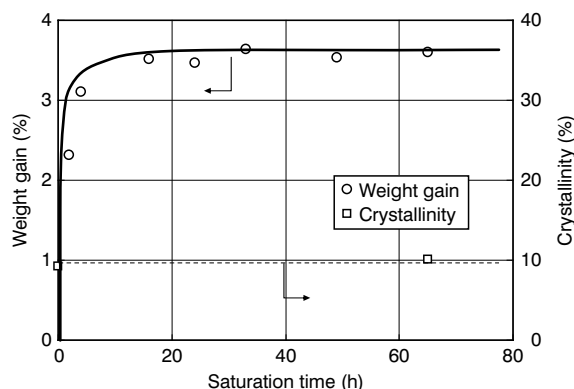


Figure 8 Effect of gas saturation time on the change in crystallinity of PPS sheet.

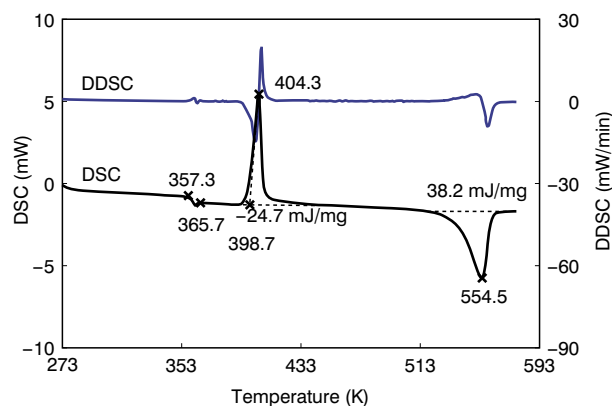


Figure 9 DSC chart for as-received PPS sheet.

completion of the foaming process at various foaming temperatures. In this experiment, in order to carry out a more accurate observation, the gas saturation pressure was set to 4.0 MPa while lowering the gas concentration before foaming, and the samples for observation of the initial stage of foaming was prepared in such a way that after the sample saturated with gas was heated for 10 sec it was quenched to prevent cell growth. The results show that, while at 373 K and 383 K secondary microcells of the submicron scale were not generated in both the initiation and completion of foaming, at 393 K and higher such secondary microcells were generated during the cell growth process, and that at 423 K the secondary microcells were already generated in 10 sec.

Accordingly, we proceeded to confirm the cell nucleation and growth process in more detail selecting the foaming temperature as 393 K and 403 K. Figure 11 shows the changes in cell morphology as the foaming time was changed from 6 sec through 60 sec. Each sample was prepared by heating for the specified foaming time followed by quenching after foaming. The results show that the secondary microcells were generated during the cell growth process at both 393 K and 403 K, and that as compared with the sample foamed at 393 K, the one foamed at 403 K indicates a shorter time in having the secondary microcells.

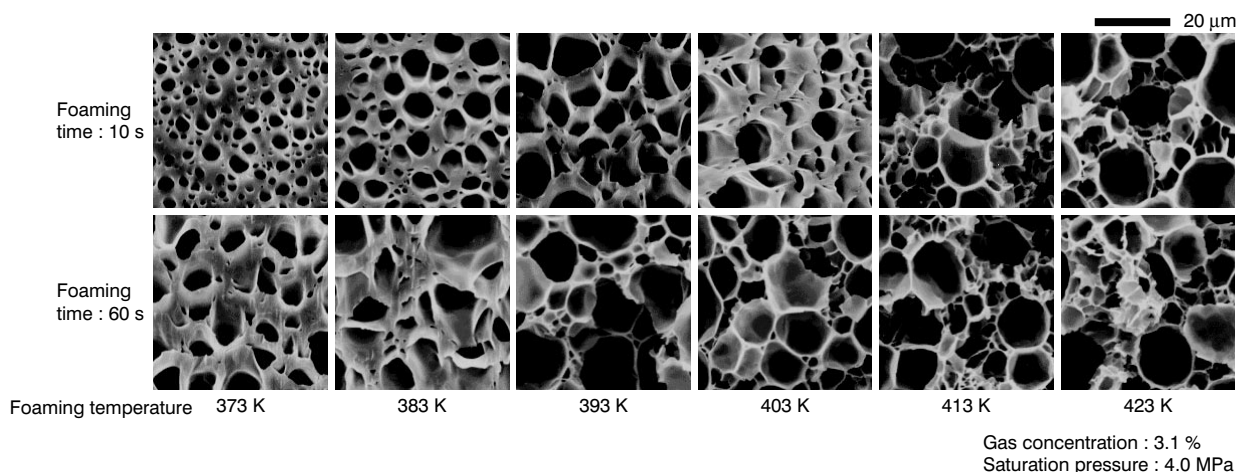


Figure 10 Cell morphology in the initiation and completion of foaming process at various foaming temperatures.

5.2 Relationship between the Cell Morphology and Crystallinity Changes

The experimental results above mentioned demonstrate that the secondary microcells are generated during the cell growth process of microcellular foaming, and suggest that, as shown in Figure 7, the secondary microcellular foaming is based on crystallization of PPS. Accordingly, in order to confirm this phenomenon in more detail, we measured using DSC the crystallinity of the foamed samples shown in Figure 11 having different foaming times to understand its change in crystallinity during the cell growth process. The results are shown in Figure 12, and as can be clearly seen, crystallization is induced by heating in the foaming process, and the secondary microcells are generated due to the crystallization.

We investigated the cell growth process and the change in crystallinity for a wider range of foaming temperatures. Three temperatures of below the crystallization temperature of PPS (373 K), near the crystallization temperature (473 K) and near the melting temperature (473 K) were selected as the foaming temperature, and the results are shown in Figure 13. When foamed below the crystallization temperature crystallization does not occur during the cell growth resulting in a unimodal cell distribution, while when foamed near the crystallization temperature crystallization occurs during the cell growth process accompanied by secondary microcells. When foaming is carried out at a higher temperature, it can be confirmed that crystallization proceeds in a very short time and that it is accompanied by immediate secondary microcellular foaming.

From these results, it may be concluded that the generation of secondary microcells is caused by the PPS crystals generated during the cell growth process.

5.3 Hypothesis about the Microcellular Foaming Behavior of PPS

A hypothesis about the microcellular foaming behavior of PPS is made from the results mentioned heretofore, which is illustrated in Figure 14 with foaming time repre-

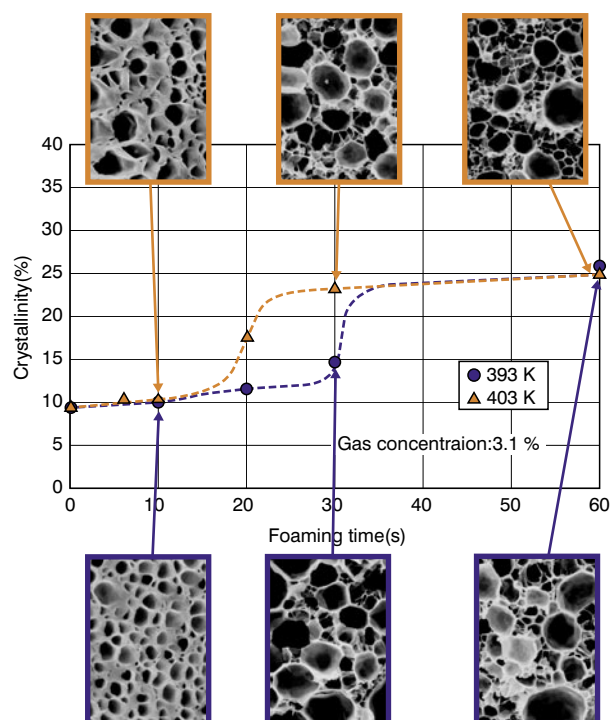


Figure 12 Relationship between the crystallinity of PPS and cell morphology (I).

sents the cell growth process on the X-axis and foaming temperature on the Y-axis. It is thought that, below the crystallization temperature, cell nucleation occurs when the temperature of the gas saturated sample goes beyond the glass transition temperature, and that the cells grow as the gas around the cell nuclei diffuses toward the nuclei. When foaming proceeds above the crystallization temperature, while, just as is the case with the foaming process below the crystallization temperature, cell nucleation occurs when the temperature goes beyond the glass transition temperature whereby the cells grow as the gas around the cell nuclei diffuses toward the nuclei, there occurs crystallization when the temperature goes beyond the crystallization temperature. At this time, it is

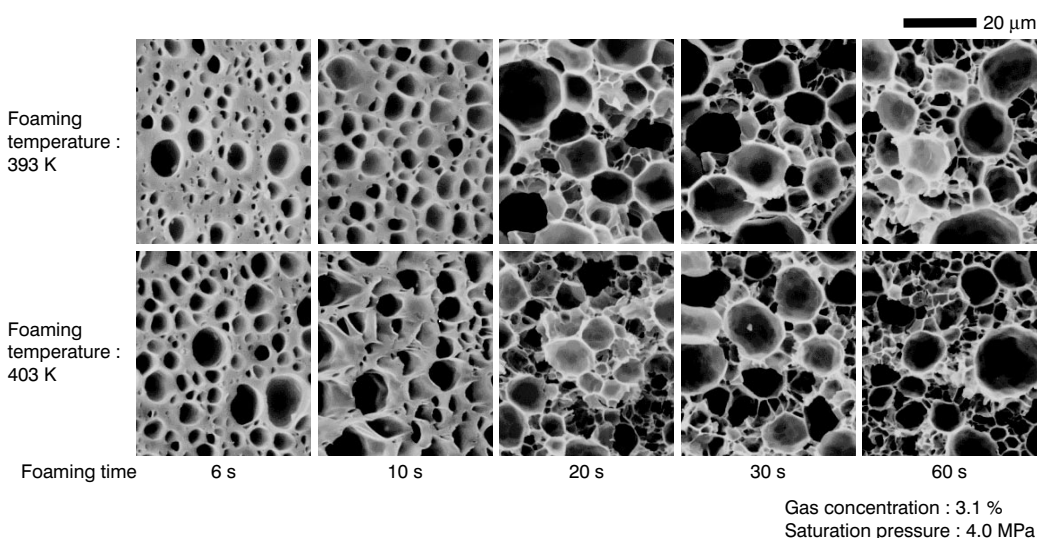


Figure 11 Cell morphology changes during the cell growth process at various foaming times.

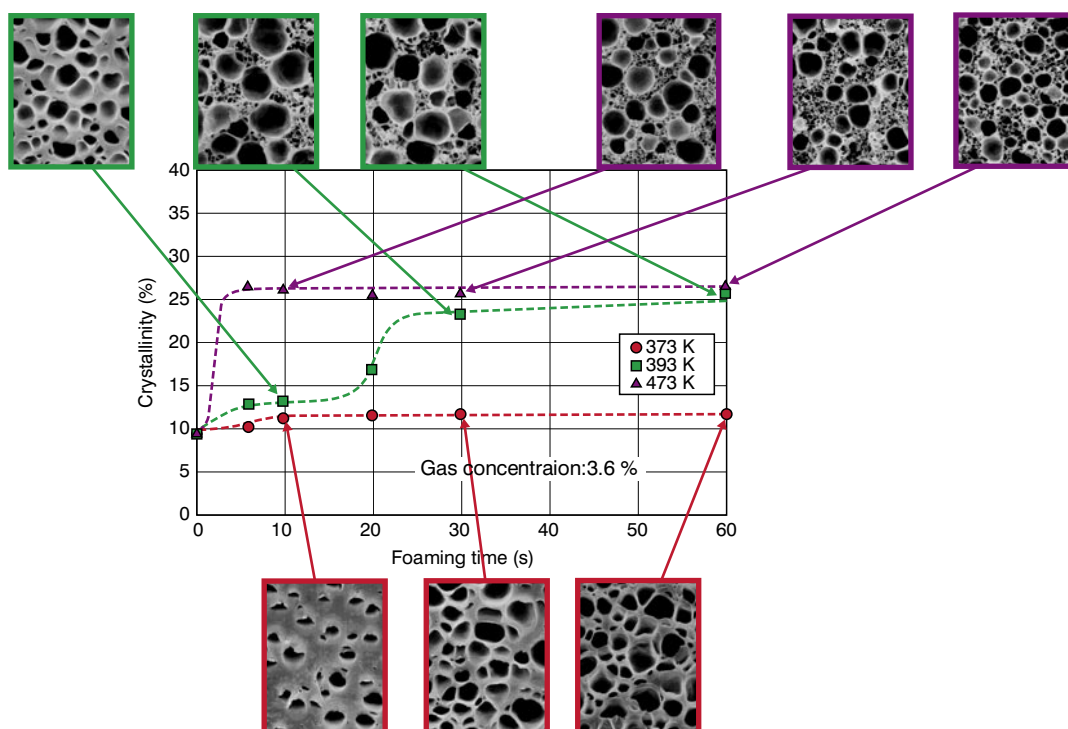


Figure 13 Relationship between the crystallinity of PPS and cell morphology (II).

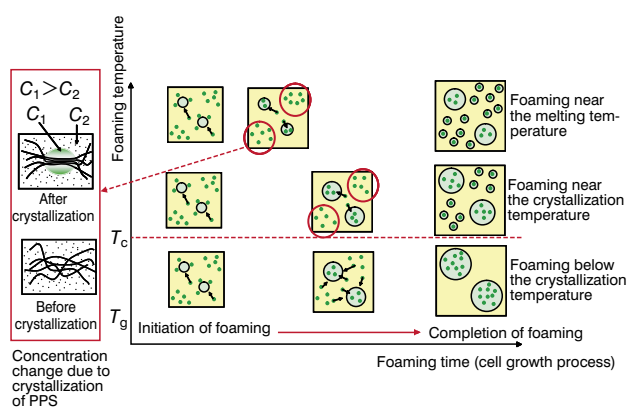


Figure 14 Hypothesis about the microcellular foaming behavior of PPS.

thought, secondary cell nucleation due to the crystallization occurs in the region that is free from cell nucleation, whereby the cells initially generated grow into the cells about $10\mu\text{m}$ in size while those due to the secondary cell nucleation become submicron-sized cells.

At a higher foaming temperature, secondary cell nucleation occurs in a shorter time due to faster crystallization, thus resulting in the generation of submicron-sized cells with a higher ratio.

With regard to the reason that the secondary cell nucleation occurs accompanied by the crystallization of PPS, it may be that the gas in the vicinity of crystallized areas is pushed out into the surroundings as crystallization proceeds resulting in a higher gas concentration in the surroundings thus enhancing cell nucleation.

6. CONCLUSIONS

The microcellular foaming behavior of PPS has been investigated, and it has been observed that the foaming behavior below the crystallization temperature is different from that above the crystallization temperature. In particular, it has been shown that the submicron-sized cells observed are generated by the cell nucleation induced by crystallization of PPS. The present study is insufficient in terms of such issues as discussions from the chemical kinetics standpoint and the relationship between crystalline morphology and cell shape. We intend to address these issues in quantitative terms in the future, ultimately promoting this study toward the ultra-microcellular foaming technology.

REFERENCES

- 1) J. E. Martin, N. P. Suh and F. A. Waldman: U. S. Patent 4473665 (1982)
- 2) F. A. Waldman: M. Thesis in Mechanical Engineering, M. I. T., January (1981)
- 3) V. Kumar and K. A. Seeler: SPE Technical Papers, 39 (1993) 1823.
- 4) M. Shimpo, D. F. Baidwin and N. P. Suh: Seikei Kako Journal, 6 (1994) 863. (in Japanese)
- 5) J. L. Hedrick et al.: Polym. Prepr., 37 (1996) 156.
- 6) A. Kabumoto: Seikei Kako Journal, 11 (1999) 966. (in Japanese)
- 7) J. E. Martini: M. Thesis in Mechanical Engineering, M. I. T., January (1981)
- 8) S. K. Goel and E. J. Beckman: Polym. Eng. Sci., 34, 14 (1994) 1137.
- 9) J. E. Weller and V. Kumar: SPE ANTEC., 55th, 2 (1997) 2037.
- 10) M. Itoh, A. Kabumoto, N. Yoshida and M. Okada: ASME, MID-Vol.53 (1994) 139.

- 11) T. Mizumoto et al.: Seikei Kako Symposia, B208 (2000) 211. (in Japanese)
- 12) J. S. Colton and N. P. Suh: Polym., Eng., Sci., 27 (1987) 485.
- 13) J. E. Martini: M. Thesis in Mechanical Engineering, M.I.T., January (1981)
- 14) K. Makino: Seikei Kako Journal, 12 (2000) 99. (in Japanese)
- 15) J.S. Colton: Ph. D. Thesis in Mechanical Engineering, M.I.T., September (1985)
- 16) E. Maemura et al.: Polymer Eng. Sci., 29 (2) (1989) 140.